JOURNAL OF MATERIALS SCIENCE 16 (1981) 787–799

Effect of CeO_2, MgO and Y_2O_3 additions on the sinterability of a milled Si_3N_4 with 14.5 wt% SiO_2

ALAN ARIAS
Lewis Research Centre, Cleveland, Ohio 44135, USA

Specimens of milled α-Si_3N_4 with 0 to 5.07 equivalent per cent of CeO_2, MgO or Y_2O_3 additions were pressureless sintered at 1650 to 1820° C for 4 h in static nitrogen at 34.5 kPa (5 psi) gauge pressure and while covered with a mixture of Si_3N_4 + SiO_2 powders. The density – per cent addition – temperature plots showed maxima which, for all three additives, occurred between ~ 1.2 and 2.5 equivalent per cent. Maximum densities resulted on sintering in the 1765 to 1820° C range and were 99.6 per cent of theoretical with 2.5 equivalent per cent CeO_2, 98.5 per cent of theoretical with ~ 1.24 to 1.87 equivalent per cent MgO, and 99.2 per cent of theoretical with 2.5 equivalent per cent Y_2O_3. Also, densities $\geqslant$ 94 per cent of theoretical were obtained with as little as 0.62 equivalent per cent additive (1.0 MgO, 2.11 CeO_2 or 1.85 Y_2O_3, in wt %). X-ray diffraction showed that the materials were predominantly β-Si_3N_4 with some or no Si_2N_2O. Scanning electron photomicrographs showed microstructures of elongated grains with aspect ratios of about 5, with all additives.

1. Introduction

Silicon nitride (Si_3N_4) base ceramics have physical and chemical properties that make them prime candidates for applications in advanced heat engines and in other high temperature oxidizing environments. These ceramics are usually manufactured either by nitridation of silicon powder compacts or by hot-pressing or pressureless sintering of Si_3N_4 powders. Partly because it allows near net-shape manufacturing of ceramics, pressureless sintering has received a great deal of attention in recent years despite the fact that this process also has some disadvantages. The main disadvantage of the pressureless sintering of Si_3N_4 is that the process requires sintering aids or additives [1–8] of the type and/or amounts that may be hazardous to health (such as Be_3N_2 additions [8]) or detrimental to the high temperature mechanical properties of the Si_3N_4 base ceramics [6, 7, 9–11]. It was surmised that low amounts of sintering aids might yield Si_3N_4 base ceramics with improved high temperature properties, provided these ceramics could be sintered to high densities. It was also surmised that the use of Si_3N_4 powders milled to a fine particle size might well provide the required sinterability with low amounts of additives, as was done in a previous investigation with sialons [9, 12].

The main objective of the present investigation was to determine the effects of additions of cerium oxide (CeO_2), magnesium oxide (MgO) and yttrium oxide (Y_2O_3) as well as the effect of sintering temperature on the sinterability of milled α-Si_3N_4. To attain this objective, equivalent amounts of these three oxides were separately mixed with milled α-Si_3N_4, cold-pressed and sintered. Various levels of oxide additions and sintering temperature were investigated to determine the effects of these variables on sinterability. The compositions investigated are indicated in the phase diagrams of Fig. 1. The sinterability was determined by density measurements, weight and dimensional changes, optical and electron microscopy and X-ray diffraction analysis of the sintered specimens.

0022–2461/81/030787–13$03.30/0

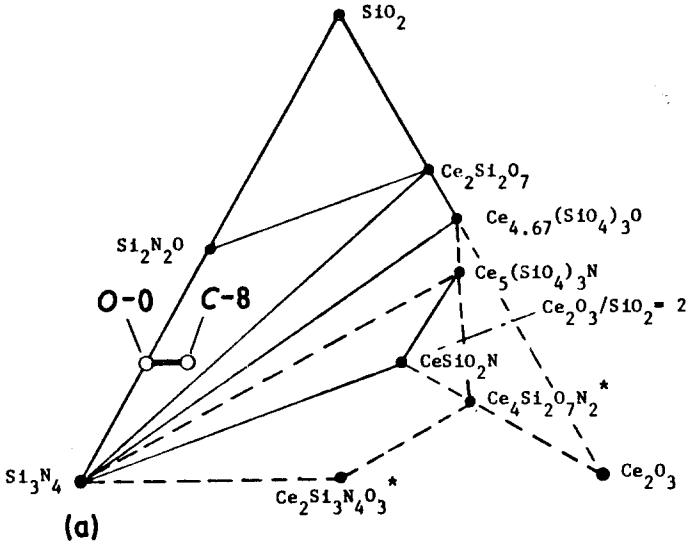

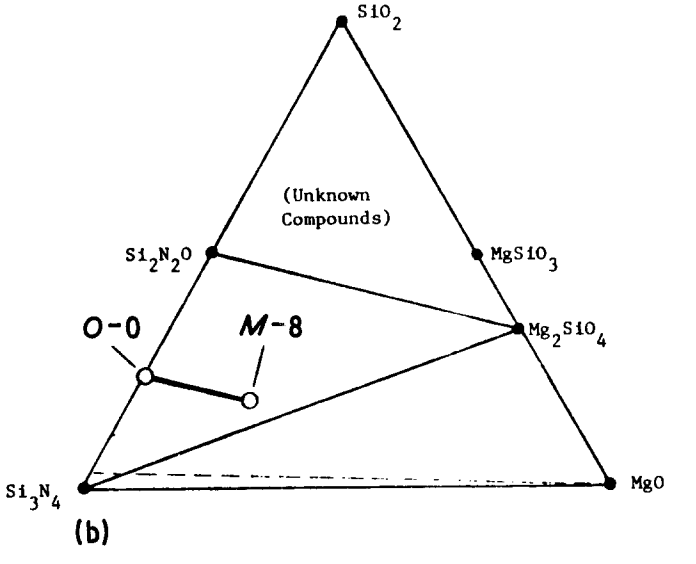

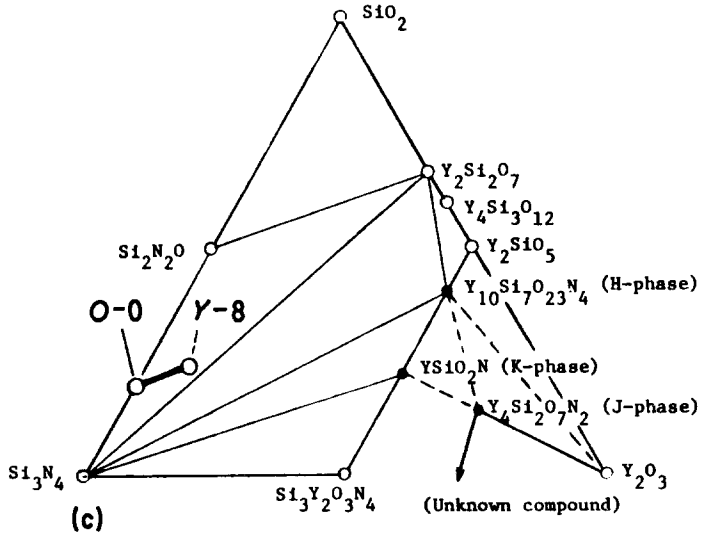

Figure 1 Phase diagrams for the systems (a) Si_3N_4–SiO_2–Ce_2O_3 [16], (b) Si_3N_4–SiO_2–MgO [19] and (c) Si_3N_4–SiO_2–Y_2O_3 [20] showing location of compositions investigated (*O*-0 to *C*-8, *O*-0 to *M*-8 and *O*-0 to *Y*-8, respectively).
*Expected but not observed.

2. Materials

The materials used in this investigation were α-Si_3N_4, CeO_2, MgO and Y_2O_3. These materials are characterized in Table I. The α-Si_3N_4 and the CeO_2 were ball milled (as outlined in Table I and in more detail in Section 4). The MgO and Y_2O_3 were used essentially as-received from the suppliers.

3. Equipment

Two types of ball mills were used in this investigation: nickel lined ball mills of 1500 cm^3 capacity with ~ 3700 g nickel shot (0.63 to 1.27 cm diameter), and type 430 stainless steel ball mills of 1500 cm^3 capacity with ~ 2500 g of type 304 stainless steel balls (1.27 cm diameter). The rest of the equipment used in this investigation (presses, cold-pressing dies, furnaces, analytical equipment, etc.) was standard laboratory equipment.

4. Procedures

The procedures used for the preparation of the powders used for compounding the Si_3N_4 base ceramics are described briefly in Table I and in more detail below. The preparation of specimens from these powders is described in more detail below.

4.1. Milling

The α-Si_3N_4 was milled in 200 g batches in the nickel lined ball mills. Water was used as the milling fluid. As already pointed out by Arias [12], during milling of the α-Si_3N_4 there is a pressure build up in the mill caused by hydrogen evolution resulting from the reaction of free silicon (in the α-Si_3N_4 used here) with water. The CeO_2 was dry milled in the stainless steel mills for 24 h. The MgO and Y_2O_3 were not milled.

4.2. Removal of pick-up

During ball milling, materials resulting from wear of balls and mills (pick-up) contaminate the powders. The effects of the pick-up on sinterability are unknown, and for this reason it was removed whenever feasible. Most of the nickel pick-up from the milled α-Si_3N_4 was removed magnetically, after separating the slurries from the nickel shot by sieving. The slurries were stirred while heating them, treated with 100 g of reagent grade nitric acid and then centrifuged to remove most of the liquid. The resulting moist powder was washed by stirring with heated distilled water. The wash water was then removed by centrifuging. The washing–centrifuging procedure was repeated twice more. The resulting powder cakes were vacuum dried at about 100° C and pulverized in a Waring blendor. The dry powders were kept in airtight containers until ready for use.

The dry-milled CeO_2 powder was separated from the balls by sieving. No attempt was made to remove the (stainless steel) pick-up from this powder because the pick-up was relatively small (see analysis in Table I) and, in addition, CeO_2 is soluble in most acids suitable for leaching out the stainless steel. After drying in air at about 100° C the dry-milled CeO_2 as well as the other two oxides were stored in airtight containers until ready for use.

4.3. Chemical and BET analyses

The powders listed in Table I were analysed for carbon and (spectrographically) for trace elements. The milled α-Si_3N_4 was also analysed for oxygen (after mixing with the temporary binder and heating at 450° C in N_2 as indicated in Sections 4.4 and 4.6 below) by the inert gas fusion method. The specific surface areas of the powders were determined by the BET (Brunauer, Emmett and Teller) method.

4.4. Mixing

The milled α-Si_3N_4 and the oxide additives making up the compositions investigated were weighed in an analytical balance. Each batch was placed in a polyethylene bottle with about twice its weight in type 304 stainless steel balls, 70 wt % anhydrous ethanol and 5 wt % DC-705 silicone oil (as temporary binder). Each batch of powder was mixed for 1 h at 100 rpm. The resulting slurry was dried with constant stirring at about 100° C. After removing the balls, the resulting powder agglomerates were broken up in a Waring blendor.

The amounts of oxide additive used in each batch are shown in Table II. In this table the amounts of additives are stated in weigth and equivalent per cent. The equivalent per cent was calculated from the number of chemical equivalents of each component in the batches (additive, α-Si_3N_4 and SiO_2 in the α-Si_3N_4). This method of reporting compositions in equivalent per cent is the same as that used in reciprocal salt systems and is described in [13, 14]. For calculation purposes, the normal valences of the elements (O^{-2}, N^{-3}) were used.

In the present investigation, batches of α-Si_3N_4

TABLE I Materials characterization

Material	Source and designation	Milling data				Post-milling treatment	Specific surface of powder ($m^2 g^{-1}$)	Chemical analysis*		
		Mill material	Balls material	Milling fluid	Milling time (h)			Oxygen (wt%)	Carbon (wt%)	Other elements, ppm unless noted otherwise (spectrographic analyses)
α-Si_3N_4	Kawecki-Berylco Industries CP-85	Ni	Ni	Water	300	Leach centrifuge, wash, centrifuge, dry	22.9	7.72†	0.20 0.49†	0.4 wt% Al-540 Ca-200 Cr-30 Cu-0.1 wt% Fe-80 Mg-70 Mn-180 Mo-240 Ni-230 Ti-140 Zr- Si major
CeO_2	Cerac Pure, C-1064	Stainless steel	Stainless steel	Air	24	None	35.4	–‡	0.019	340 Ca-0.2 wt% Cr-0.3 wt% Fe-250 Mg-630 Mo-450 Ni-Ce major
MgO	Fisher Scientific, M-300	–	–	–	0	–	19.6	–‡	0.675	130 Al-0.2 wt% Ca-200 Fe-Mg major-120 Mn-840 Si-80 Ti
Y_2O_3	Research Chemicals, 99.9% pure	–	–	–	0	–	69.9	–‡	0.144	50 Al-75 Ca-<10 Co-2 Cr-<50 Cu-<20 Fe-<5 Mn-<20 Mo-2000 Na-<100 Nb-5 Ni-<100 Pb-<50 Sn-5 Ti-<10 V-<40 W- Y major-<10 Zr

*Analyses of materials used for compounding batches.
†These carbon and oxygen contents were obtained after mixing for 1 h with 5 wt% silicone oil and 70 wt% ethanol, then heating at 450° C for 1 h in flowing nitrogen.
‡Not determined.

TABLE II Compositions investigated and designations

Additive	Designation	Composition of mixture	
		Weight per cent*	Equivalent per cent†‡
None	*O*-0	0	0
MgO	*M*-0.5	0.500	0.308
	M-1	1.000	0.617
	M-2	2.000	1.238
	M-3	3.000	1.865
	M-4	4.000	2.496
	M-6	6.000	3.773
	M-8	8.000	5.071
CeO_2	*C*-1	2.110	0.617 (0.463)
(Ce_2O_3)‡	*C*-2	4.174	1.238 (0.932)
	C-3	6.192	1.865 (1.405)
	C-4	8.167	2.496 (1.884)
	C-6	11.990	3.773 (2.857)
	C-8	15.654	5.071 (3.852)
Y_2O_3	*Y*-1	1.851	0.617
	Y-2	3.670	1.238
	Y-3	5.458	1.865
	Y-4	7.217	2.496
	Y-6	10.647	3.773
	Y-8	13.966	5.071

*In mixture before sintering.
†Calculated composotion after sintering, assuming reaction of 0.49 wt% carbon with SiO_2 to form SiO and CO.
‡Data for Ce_2O_3 in parenthesis. The equivalent per cent was calculated on the assumption that CeO_2 reacts with Si_3N_4 to form SiO_2 and N_2.

with the same equivalent per cent of the various additives were used to facilitate comparisons of the effect of additives on sinterability.

4.5. Cold-pressing

The powder mixtures were shaped into bars approximately 3.18 cm x 0.79 cm x 0.39 cm in a double acting steel die at a pressure of 207 MPa (30×10^3 psi). These bars were encased in plastic bags which were then evacuated, sealed and isostatically cold-pressed at 483 MPa (70×10^3 psi).

4.6. Removing the fugitive binder

The silicone oil binder was removed from the cold-pressed bars by heating them in flowing nitrogen at 450° C for 1 h.

4.7. Sintering

The bars to be sintered were measured and weighed. These bars were placed in a graphite boat and packed all around with a mixture of as-received α-Si_3N_4 and 5 wt%, 325 mesh, 99.9% pure SiO_2 [12]. A new batch of this powder pack was used for each sintering run. Each sintering run at a given temperature normally included one bar of each composition investigated. All sintering runs were carried out in a furnace with graphite heating elements and under an atmosphere of static nitrogen at 34.5 kPa (5 psi) gauge pressure. The temperature range investigated was from 1650 to 1820° C and the time at temperature was 4 h in all cases. The sintering temperatures were monitored and controlled with W/W-26 Re thermocouples. After sintering, the bars were sandblasted.

4.8. Characterization

The sintered and sandblasted bars were weighed and measured to determine weight loss and shrinkage. The density of these bars was determined either from their dimensions and weights or by water immersion depending on whether or not they were porous. Some of these bars were then either cut or broken into pieces suitable for optical microscopy, scanning electron microscopy (SEM) or X-ray diffraction analyses.

4.9. Hot-pressing

Mainly to compare densities, some of the compositions were also hot-pressed. Hot-pressing was done in a double acting graphite die at 1750 ± 25° C and 27.6 MPa (4000 psi) for 30 min in flowing nitrogen. The resulting bars were assumed to be 100% dense. The as hot-pressed densities were then used to calculate the theoretical densities of the pressureless sintered bars.

5. Results and discussion

5.1. Compositions and temperature range investigated

The three oxide additives (CeO_2, MgO and Y_2O_3) used in the present investigation were selected for study, from among the many high melting point oxides available, as a result of some preliminary work at NASA [14] and also because published results [11, 15] showed that CeO_2, MgO and Y_2O_3 had been found satisfactory as hot-pressing aids for Si_3N_4.

In Table II the compositions used in this investigation are listed together with their designations, wt% additive and equivalent per cent additive. Each composition in the table is designed by a letter (*M* for MgO, *C* for CeO_2 and *Y* for Y_2O_3) and a numeral. For compositions containing MgO, this numeral is also the wt% of MgO in the original

mixture compounded from the materials in Table I. For the compositions containing the other oxides the numeral in their designation does not correspond with their wt% additive. However, all compositions having the same numeral in their designation contain the same equivalent per cent of oxide additive. The equivalent per cent shown in Table II was calculated on the assumption that the carbon remaining after removing the fugitive binder (Table I) reacted with about 2.5 wt% of the original 14.5 wt% SiO_2 in the milled α-Si_3N_4 to form SiO and CO gases during sintering. As shown in Table II, the amounts of additives used ranged from 0 to 5.071 equivalent per cent.

Batches containing one bar from each of the compositions listed in Table II were sintered at 1700, 1735, 1765 and 1820° C. In addition, one batch containing only one bar from each of the MgO compositions (*M*-0.5 to *M*-8) was sintered at 1650° C.

Attempts were made to calculate the per cent of theoretical densities on the bases of the calculated theoretical densities of the sintered bars. However, in some instances the calculated per cent of theoretical density was found to be in excess of 100. For this reason, some of the compositions were hot-pressed to obtain more meaningful baseline densities.

5.2. Hot-pressed densities

Fig. 2 shows the densities of hot-pressed (HP) Si_3N_4 containing 0.617, 2.496 and 5.071 equivalent per cent of each of the three oxide additives used in the present investigation. Milled α-Si_3N_4 without additives was found to be quite porous after hot-pressing and the corresponding data point is not used. Instead the theoretical density of the milled α-Si_3N_4 was calculated on the assumption that during sintering the carbon in α-Si_3N_4 reacts with a SiO_2 to form SiO and CO [9, 12]. It was also assumed that the remaining SiO_2 forms Si_2N_2O (density = 2.85 g cm^{-3}). On these bases, the fully dense Si_3N_4 of Table I with no additives would have a density of 3.04 g cm^{-3} which is the value plotted in Fig. 2. As this figure shows, the densities of the hot-pressed compositions extrapolate quite well to 0% additive.

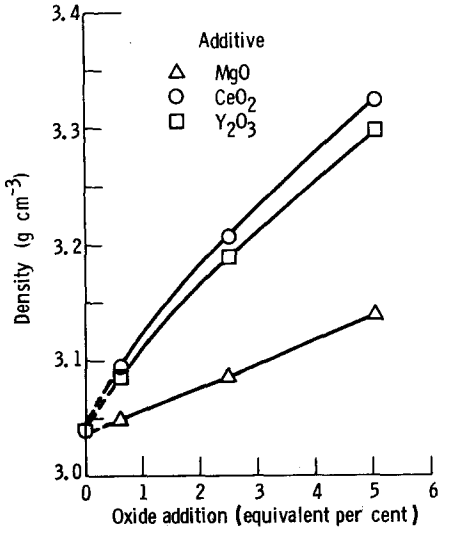

Figure 2 Densities of Si_3N_4 with oxide additions after hot pressing at 1750° C and 27.6 MPa (4000 psi) for 30 min.

5.3. Effect of composition and sintering temperature on density

Fig. 3 shows the effect of MgO additions and sintering temperature on the density of pressureless sintered Si_3N_4. At all sintering temperatures, the density increases steeply with increasing MgO additions near the origin of the plots. As a rule, the higher the sintering temperature the steeper this density increases, except perhaps for the 1650° C plot, whose density near the origin is unknown because the data point for 0% MgO is missing. After the initial steep increase in density the steepness of the plots gradually decreases,

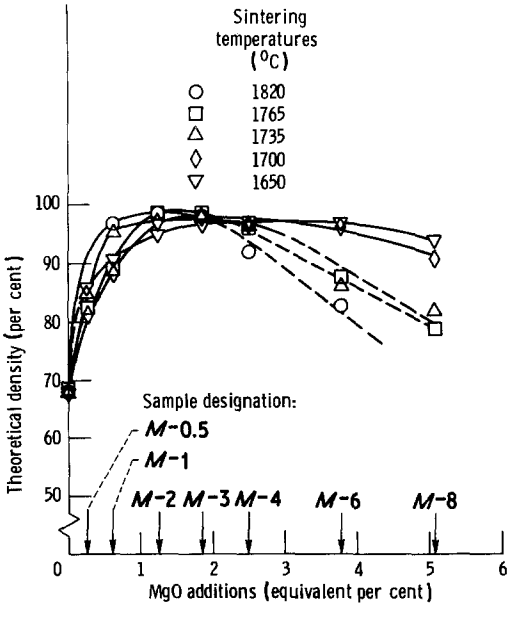

Figure 3 Effect of MgO additions and sintering temperature on density of pressureless sintered Si_3N_4. (All samples sintered 4 h in N_2).

the density reaches a maximum between about 0.93 and 1.87 equivalent per cent (1.5 to 3 wt%) MgO, then the density decreases with increasing MgO. In most cases, this decrease in density with MgO in excess of about 1.87 equivalent per cent was accompanied by bloating. Maximum densities of about 98.5% of theoretical were obtained by sintering compositions with 1.24 to 1.87 equivalent per cent (2 to 3 wt%) MgO. As a rule, the higher the sintering temperature the lower the amount of MgO at which maximum density occurred. As the plots indicate, it was possible to obtain materials with 96% or better of their theoretical densities by sintering at high temperatures (1765 to 1820° C) with as little as 0.62 equivalent per cent (1 wt%) MgO. These are the highest densities so far reported in the literature for pressureless sintered Si_3N_4 with such small amounts of additive. Sintering at lower temperatures (1650° C) with 1.55 to 4.42 equivalent per cent (2.5 to 7 wt%) MgO also gave densities in excess of 96% of theoretical.

Fig. 4 shows the effects of CeO_2 additions and sintering temperature on the density of pressureless sintered Si_3N_4. Although the data in Fig. 4 is presented in terms of CeO_2, it may be noted that during sintering the CeO_2 reacts with Si_3N_4 to form Ce_2O_3, SiO_2 and N_2 [16]. The corresponding, calculated equivalent per cent Ce_2O_3 is nearly 3/4 that of CeO_2, even taking into account the loss of N_2 and the additional SiO_2 formed. These equivalent per cent Ce_2O_3 are shown in parenthesis in Table II. However, and as will be shown later on, because of material transfer, decomposition and glass formation the compositions of the sintered materials can only be surmised. For these reasons and for the sake of consistency, the data in Fig. 4 is presented in terms of CeO_2. As shown in Fig. 4, the density increases with increasing additive, reaches a maximum and then declines. In this case, however, the maxima all occur at about 2.5 equivalent per cent (8.17 wt%) CeO_2 (or 1.9 equivalent per cent Ce_2O_3). Beyond this value all compositions sintered about equally well at all temperatures investigated, but the density decreased with increasing CeO_2. As the plots show, it was possible to sinter these compositions to 95% of theoretical density with as little as 0.62 equivalent per cent (2.11 wt%) of CeO_2 (or 0.46 equivalent per cent Ce_2O_3). In this system, the maximum density was 99.6% of theoretical and was obtained at 2.5 equivalent per cent (8.17 wt%) of CeO_2 (or 1.9 equivalent per cent Ce_2O_3) and 1765 to 1820° C.

Fig. 5 shows the effect of Y_2O_3 additions and sintering temperatures on the density of pressureless sintered Si_3N_4. Here again, the plots show maxima at about 2.5 equivalent per cent (7.22 wt%). For this system the maximum density obtained was 99.2% of theoretical at 2.5 equivalent per cent and 1765 to 1820° C. In general, in the lower temperature range (≤ 1735° C) compositions containing Y_2O_3 did not sinter as well as those with CeO_2 or MgO. However, in the high temperature sintering range (> 1735° C) it was possible to obtain densities ≥ 94% of theoretical with as little as 0.62 equivalent per cent (1.85 wt%) Y_2O_3.

From the above it may be concluded that the maximum densities obtainable on sintering with

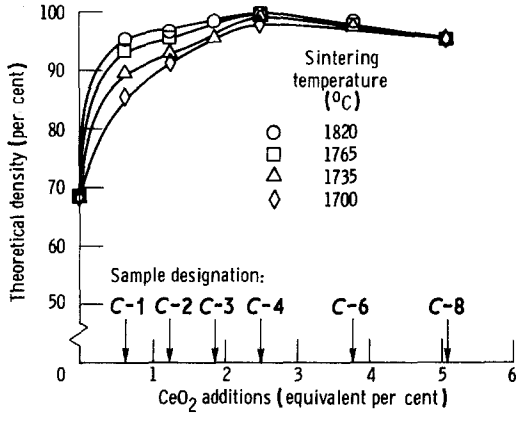

Figure 4 Effect of CeO_2 additions and sintering temperature on density of pressureless sintered Si_3N_4. (All samples sintered 4 h in N_2).

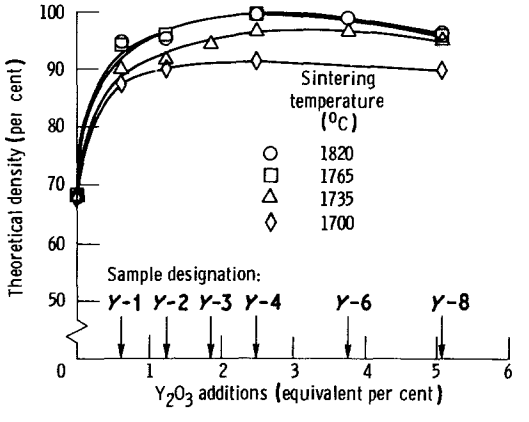

Figure 5 Effect of Y_2O_3 additions and sintering temperature on density of pressureless sintered Si_3N_4. (All samples sintered 4 h in N_2).

MgO, CeO_2 and Y_2O_3 additives are about the same, within the limits of experimental error. However, either on a wt% or equivalent per cent basis, MgO is a more effective sintering aid than either CeO_2 or Y_2O_3. On an equivalent per cent basis, CeO_2 and Y_2O_3 are about equally effective as sintering aids, except that CeO_2 is somewhat more effective than Y_2O_3 at temperatures below about 1735° C. It is surmised that the reason for this is that the Ce_2O_3 formed during sintering has a melting point of about 1690° C and pressumably forms a liquid phase with SiO_2 at a lower temperature than Y_2O_3 does.

The high sinterability of the compositions investigated is attributed mainly to the very fine particle size of the powders (Si_3N_4–SiO_2 and additives) used. Fine powders are believed to facilitate the formation of the glass required for liquid phase sintering. The fact that the glass former (SiO_2) is readily available everywhere throughout the powder compact as a coating on the Si_3N_4 quite probably contributes to the speed of glass formation and, therefore, sinterability. It is not possible to discuss herein the relative merits of the various possible glasses as liquid phase sintering aids because their properties (such as viscosity and surface tension) are unknown. Further, as will be shown later, most of the compositions not only contain undetermined amounts of Si_2N_2O but also gain or loose weight due to decomposition, reactions and material transfer during sintering. Therefore, the amounts and compositions of the glasses formed during sintering are unknown and, for these reasons, conclusions regarding the effects of the various additives on sinterability will be mainly based on the observed sintering behaviour.

It may be noted that the sintered density–composition plots for all three additives show a rapid increase in density with composition at the origin of the plots. From this it is concluded that small amounts of suitable additives or impurities can have a relatively large effect on sinterability. After this rapid increase in density the various compositions, particularly those sintered at or above 1765° C, reach maximum density within the range of about 1 to 4 equivalent per cent and then the density decreases with increasing additive beyond about 4 equivalent per cent. It is theorized that this decrease in density results from gas bubbles (SiO and N_2 due to reactions) forming more easily in the increasingly more fluid glass resulting from increasing amounts of sintering aid. It is also theorized that gas bubble formation is suppressed by the pressure applied during hot pressing and that, therefore, the hot-pressed density is a better measure of the true density.

The fluidity of the glass formed probably also has an effect on other high temperature properties that depend on material transport, such as creep strength and oxidation resistance, which should increase with decreasing glass fluidity. In this context, it can be seen in the plots of Figs 3 to 5 that at low sintering temperature (~ 1700° C) MgO is a better sintering aid than CeO_2 and this, in turn, better than Y_2O_3 and since increasing sinterability results (at least in part) from a more fluid glass it is surmised that high temperature creep strength and oxidation resistance should be better with Y_2O_3 than with either CeO_2 or MgO additions, other things being equal.

5.4. Shrinkage and weight losses

Table III lists representative linear (length) shrinkages and weight losses of compositions involving the three oxide additives at all the temperatures investigated. As shown in the table, shrinkages varied from 8.5 to 13.5% but the best sintered specimens (density > 98% of theoretical) showed shrinkages from about 12 to 13.1%. However, shrinkage alone is not a good criteria for determining sinterability, mainly because shrinkage involves the combined effects of sintering and weight losses.

In general, weight losses increase with increasing sintering temperature. This was to be expected, in view of the well known fact that Si_3N_4 both decompose and react with SiO_2 at high temperature [12, 17], and the reduction of CeO_2 to Ce_2O_3 which has already discussed. However, considering both decomposition and reaction, most of the compositions show surprisingly small weight losses, except for MgO-bearing compositions at high temperatures. These MgO-bearing compositions with high weight losses usually consisted of a dark, hard core and a light coloured coating abradable by sandblasting. However, as shown in the plots in Fig. 3 and the data in Table III, it was possible to obtain reasonably well sintered (~ 97% theoretical density) MgO-bearing compositions with very small weight losses by sintering at 1650° C. The large weight losses of these MgO-bearing compositions at high sintering temperatures are attributed to the relatively high volatility

TABLE III Shrinkage and weight losses of Si_3N_4 with oxide additives during sintering

Additive	Designation (Table II)	Sintering temperature (°C)									
		1650		1700		1735		1765		1820	
		Shrinkage (%)	Weight loss (%)	Shrinkage (%)	Weight loss (%)	Shrinkage (%)	Weight loss (%)	Shrinkage (%)	Weight loss (%)	Shrinkage (%)	Weight loss (%)
MgO	*M*-1	9.1	1.2	9.0	2.3	10.3	2.8	9.0	5.7	9.7	10.6
	M-4	12.3	0.6	11.8	3.1	12.0	3.8	12.0	10.0	12.0	11.3
	M-8	12.3	0.4	10.6	2.2	12.0	4.8	10.1	4.7	10.4	9.3
CeO_2	*C*-1	–	–	8.5	0.4	9.6	0	10.3	0.3	11.9	4.2
	C-4	–	–	12.0	1.0	12.2	0.4	12.9	1.2	12.6	1.2
	C-8	–	–	11.2	2.2	11.1	0.1	11.4	0.2	11.7	1.2
Y_2O_3	*Y*-1	–	–	9.1	1.4	10.0	− 0.3	11.5	0.9	13.1	8.9
	Y-4	–	–	10.4	0.6	12.1	− 0.2	12.2	− 0.3	13.1	1.5
	Y-8	–	–	10.3	− 0.8	11.9	− 1.1	12.4	− 0.7	12.5	− 0.6

of MgO in reducing and neutral atmospheres. On the other hand, CeO_2- and Y_2O_3-bearing compositions show very small weight losses, and some of the latter even show weight gains, up to the highest sintering temperatures used. As shown in [12], increasing the SiO_2 content of the Si_3N_4 powder pack cover not only decreased the weight losses during sintering of sialons but in some cases produced weight gains. It was found in [12] that 5 wt% SiO_2 addition to the Si_3N_4 used for powder pack cover yielded sialon bars with negligible sintering weight changes and this is the reason for using the same powder pack cover in the present investigation. It may be noted, however, that in all cases in the present investigation and in [12] the powder pack covers lost weight. From this it is theorized that there is material transport from the powder pack to the compact via the volatile SiO formed according to the reaction,

$$4Si_3N_4 + 9SiO_2 = 3Si_2N_2O + 15SiO + 5N_2.$$

Disregarding the activities of Si_3N_4, SiO_2 and Si_2N_2O, the reaction will go to the right or left, depending on whether the fugacities of SiO and N_2 are smaller or larger, respectively, than the equilibrium fugacities. In this investigation the fugacity (pressure) of N_2 is practically constant but that of SiO is not. It is surmised that the fugacity of the SiO formed in the compacts depends upon the kind and concentration of additive in the liquid phase (glass) formed during sintering. Therefore, a given compact gains or loses weight depending on whether the fugacity of the SiO resulting from the reaction of Si_3N_4 and SiO_2 in the compact is smaller or larger, respectively, than the fugacity of SiO resulting from the same reaction in the powder pack.

5.5. Microstructure

Fig. 6 shows light photomicrographs of compositions made with the three oxide additives used in this investigation and having the best obtainable densities for each kind of additive. All three photomicrographs show well sintered, relatively pore-free materials with two-phase matrices in which are embedded small amounts of a dark grey third phase as a round constituent and still smaller amounts of bright, metallic-looking specks of a fourth phase. The same four phases appear in all the compositions and at all the temperatures investigated. As a rule, the larger the amount of additive and the higher the sintering temperature the larger the amount of the dark grey phase. The metallic-looking specks are probably silicon or a silicon base alloy [12]. For reasons to be discussed in the next section, it is surmised that the matrix phases are β-Si_3N_4 and Si_2N_2O and that the dark grey phase is probably glass.

Fig. 7 shows a scanning electron photomicrograph of the fracture surface of Si_3N_4 with 2.5 equivalent per cent CeO_2 (*C*-4) after sintering at 1765° C. The specimen shown was etched in fused

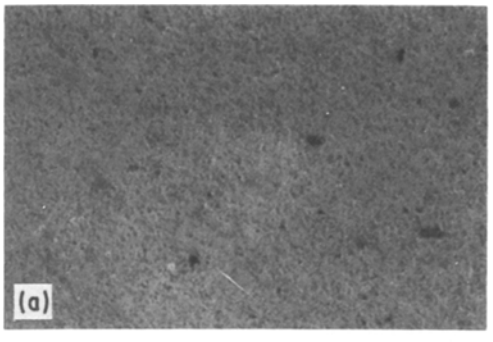

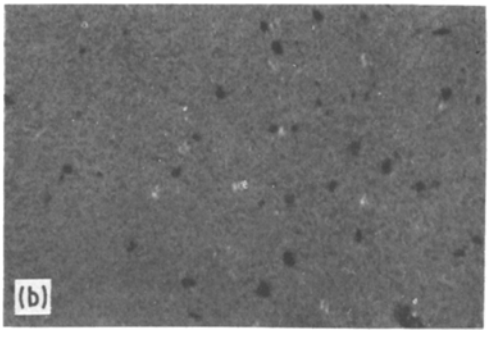

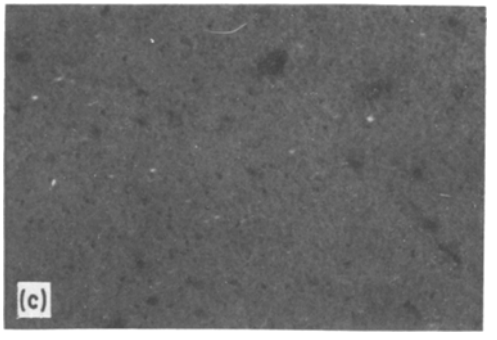

Figure 6 Light photomicrographs of Si_3N_4 base compositions with the highest densities. All compositions were pressureless sintered 4 h in stagnant nitrogen at 1765° C, unetched, (a) MgO = 1.24 equivalent per cent (*M*-2); density = 3.02 g cm^{-3}, (b) CeO_2 = 2.5 equivalent per cent (*C*-4); density = 3.20 g cm^{-2} and (c) Y_2O_3 = 2.5 equivalent per cent (*Y*-4); density = 3.16 g cm^{-3} (× 275).

40 KOH : 40 NaOH : 20 LiOH at 180° C for 30 min [8]. Although not shown, the microstructures of Si_3N_4 with 2.5 equivalent per cent of either MgO or Y_2O_3 and sintered at 1765° C are practically the same as that shown in Fig. 7. All of these etched samples showed elongated grains with an aspect ratio of about 5 and average length of about 2 μm. The grain shape and size appeared to be fairly independent of kind and amount of additive. The grain size, however, increased with increasing sintering temperature. Scanning electron photomicrographs showed that the milled α-Si_3N_4 powder was very fine and equiaxed. Therefore, the elongated grain structure was developed during sintering. The transformation of equiaxed α- to elongated β-Si_3N_4 during pressureless sintering, as found in the present investigation and by others [5, 8] may lead to Si_3N_4-base ceramic with improved bend strength and fracture toughness [18].

5.6. X-ray diffraction analysis and implications

From the chemical composition of the starting mixtures (Table II) it is possible to determine the equilibrium phases that should be present in the various sintered compositions. Thus, as shown in Fig. 1, all the CeO_2-bearing compositions investigated fell within the Si_3N_4–$Ce_2Si_2O_7$–Si_2N_2O compatibility triangle of the Si_3N_4–Ce_2O_3–SiO_2 system [16], all the MgO-bearing compositions investigated fell within the Si_3N_4–Mg_2SiO_4–Si_2N_2O compatibility triangle of the Si_3N_4–MgO–SiO_2 system [19] and all the Y_2O_3-bearing compositions investigated fell within the Si_3N_4–$Y_2Si_2O_7$–Si_2N_2O compatibility triangle of the Si_3N_4–Y_2O_3–SiO_2 system [20]. Therefore, in view of the above relationships, it was interesting to see that, as shown by the X-ray diffraction analyses in Table IV, the compositions from the present investigation were predominantly β-Si_3N_4 with small amounts of Si_2N_2O. The tridymite detected in some of the samples was probably on the sandblasted surface surrounding the ground surfaces on which the analyses were taken. Thus, despite the fact that some of the compositions (*M*-8, *C*-8 and *Y*-8, for example) have relatively large amounts of additives these were not detected (as compounds such as Mg_2SiO_4, $Y_2Si_2O_7$ etc.) by X-ray diffraction. Yet these additives must have been largely retained in the sintered materials because in most cases the percentage weight losses during sintering (Table III) were smaller than the wt % of additive used. It may also be noted that compositions with large amounts of additive (such as *M*-8, *C*-8 and *Y*-8) and sintered at high temperature show either β-Si_3N_4 alone or β-Si_3N_4 with very small amounts of Si_2N_2O. Within the limits of experimental error, the lattice parameters of these two phases appear to be constant and independent of the amount of additive. From these facts it is concluded that the additives are probably mostly in a glass phase (undetected by X-ray diffraction) and that the amount of this nitrogen-rich glass phase probably increases with the amount of additive and with sintering temperature. These views are further supported by the fact that the amount of grey phase seen in the light photomicrographs increases with increasing amount of additive. It follows that the two matrix phases seen in all the optical photomicrographs (Fig. 6) are β-Si_3N_4 and (probably) Si_2N_2O and that the dark grey phase which appears as a rounded constituent is probably a glass.

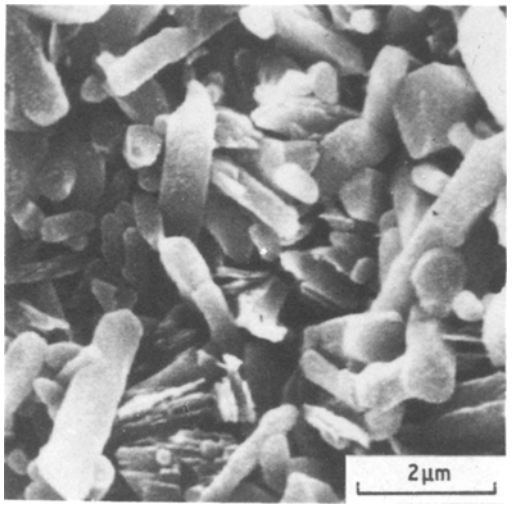

Figure 7 Scanning electron micrographs of fracture surface of Si_3N_4 with 2.5 equivalent per cent CeO_2 after pressureless sintering at 1765°C. Etched.

6. Conclusions

The present investigation was conducted to determine the effects of oxide additions and sintering temperatures on the sinterability of milled α-Si_3N_4 containing 14.5 wt % SiO_2. From the results obtained it is concluded that:

(1) CeO_2, MgO or Y_2O_3 additions can bring about densification of milled α-Si_3N_4 with 14.5 wt % SiO_2 to > 98% of theoretical density.

TABLE IV X-ray diffraction analyses of sintered Si_3N_4 with oxide additives

Additive	Designation (Table II)	Sintered at 1765° C*	Sintered at 1820° C*
MgO	*M*-4	β-Si_3N_4 = vs	β-Si_3N_4 = vs
		Si_2N_2O = vw	Si_2N_3O = vvw
	M-6	β-Si_3N_4 = vs	
		Si_2N_2O = w	–
		Tridymite = m	
	M-8	β-Si_3N_4 = vs	–
CeO_2	*C*-1	β-Si_3N_4 = vs	
		Si_2N_2O = vw	–
	C-4	β-Si_3N_4 = vs	β-Si_3N_4 = vs
		Si_2N_2O = vw	Si_2N_2O = w
			Tridymite = w
	C-8	β-Si_3N_4 = vs	β-Si_3N_4 = vs
		Si_2N_2O = vvw	
Y_2O_3	*Y*-1	β-Si_3N_4 = vs	
		Si_2N_2O = m	–
	Y-2	β-Si_3N_4 = vs	
		Si_2N_2O = m	–
	Y-4	β-Si_3N_4 = vs	
		Si_2N_2O = vvw	–
	Y-8	β-Si_3N_4 = vs	β-Si_3N_4 = vs

*m = medium; s = strong; w = weak; vs = very strong; vw = very weak; vvw = very, very weak.

However, smaller amounts of MgO are required to obtain this result.

(2) The decrease in density with increasing amounts of additive in excess of about 4 equivalent per cent probably results from increasing liquid phase fluidity with increasing additive. A more fluid liquid phase would facilitate formation of bubbles of SiO and N_2 gases from the reaction of Si_3N_4 and SiO_2 during sintering.

(3) Other things being equal, Y_2O_3-bearing compositions probably have better creep and oxidation resistance than CeO_2- or MgO-bearing compositions. This conclusion is based on the fact that at $\sim 1700°$ C Y_2O_3 is the worst sintering aid of the three, probably because the corresponding liquid phase is also the most viscous.

(4) Small amounts of suitable additives or impurities can have a relatively large effect on sinterability. This conclusion is based on the fact that the sintered density–composition plots for all three additives show a rapid increase in density with compostion at the origin of the plots.

(5) Powder pack covers of Si_3N_4–SiO_2 reduce weight losses and may even bring about weight gains in the sintered compacts because the fugacity of the SiO gas resulting from the reaction of Si_3N_4 and SiO_2 is generally lower in the compact than in the powder pack, due to the presence of the additives in the liquid phase of the compact.

References

1. K. H. JACK and W. I. WILSON, *Nature* **328** (1972) 28.
2. R. R. WILLS, *J. Amer. Ceram. Soc.* 58 (1975) 335.
3. G. R. TERWILLIGER and F. F. LANGE, *J. Mater. Sci.* **10** (1975) 1169.
4. M. MITOMO, M. TSUTSUMI, E. BANNAI and T. TANAKA, *Amer. Ceram. Soc. Bull.* **55** (1976) 313.
5. I. ODA, M. KANENO and N. YAMAMOTO, in "Nitrogen Ceramics", edited by F. L. Riley (Noordhoff, Leyden, 1977) p. 359.
6. A. W. J. M. RAE, D. P. THOMPSON and K. H. JACK, in "Ceramics for High Performance Applications II", edited by J. J. Burke, E. N. Lenoe and R. N. Katz (Brook Hill, Massachus., 1978), p. 1039.
7. J. T. SMITH, Sixteenth Highway Vehicles Systems Contractor's Co-ordination Meeting, CONF-7904105, April, 1979, Dearborn, USA, (US Dept. of Energy, Washington, 1979) p. 171.
8. S. PROCHAZKA and C. D. GRESKOVICH, "Development of a Sintering Process for High-Performance Silicon Nitride", AMMRC TR 78-32, Army materials and Mechanics Research Centre, U.S.A. (1978).
9. A. ARIAS, *J. Mater. Sci.* **14** (1979) 1353.
10. J. L. ISKOE, F. F. LANGE and E. S. DIAZ, *ibid.* **11** (1976) 908.
11. G. Q. WEAVER and J. W. LUCEK, *Amer. Ceram. Soc. Bull.* **57** (1978) 1131.
12. A. ARIAS, "Effect of Oxygen to Nitrogen Ratio on Sinterability of Sialons", NASA Report TP 1382 (1979).
13. L. J. GAUCKLER and G. PETZOW, in "Nitrogen Ceramics" edited by F. L. Riley (Noordhoff, Leyden,

1977) p. 41.
14. A. ARIAS, "Effect of Oxide Additions and Temperature on the Sinterability of milled α-Si_3N_4", NASA Report TP-1644 (1980).
15. I. C. HUSEBY and G. PETZOW, *Powder Metall. Int.* **6** (1974) 17.
16. F. F. LANGE, *Amer. Ceram. Soc. Bull.* **59** (1980) 239.
17. K. H. JACK, *J. Mater. Sci.* **11** (1976) 1135.
18. G. HIMSOLT, H. KNOCH, H. HUEBNER and F. W. KLEINLEIN, *J. Amer. Ceram. Soc.* **62** (1979) 29.
19. F. F. LANGE, *ibid.* **61** (1978) 53.
20. F. F. LANGE, S. C. SINGHAL and R. C. KUZNICKI, *ibid.* **60** (1977) 249.

Received 30 April and accepted 2 September 1980.